Color Constancy in a Rough World

Qasim Zaidi

State University of New York, College of Optometry, 33 West 42nd Street, New York, NY 10036

Abstract: This article introduces a new psychophysical method for a performance-based view of color constancy, in which the task for the observer is to identify similar materials across illuminants despite possible appearance changes, and to simultaneously extract the relative colors of the illuminants.[15] The article also examines generality conditions for the task. Physical and neural constraints on chromatic signals make it possible to use simple affine-heuristic algorithms to solve the correspondence problem for most Lambertian surfaces in random spatial arrangements under different illuminants. For rough surfaces, where the relative amounts of interface and body reflections vary with source-object-sensor geometry, the algorithms solve the correspondence problem across illuminants for a constant source-object-sensor geometry, but are not successful for rough surfaces in different spatial arrangements under different illuminants. © 2000 John Wiley & Sons, Inc. Col Res Appl, 26, S192–S200, 2001

Key words: color constancy; color identification; natural scenes

INTRODUCTION

By selectively absorbing wavelength bands of electro-magnetic radiation in specialized photoreceptors and performing neural operations on the resulting signals, the human brain creates the percept we call color. It is obvious that this percept is a major contributor to visual aesthetics, but does it also serve any utilitarian purposes? A large number of articles have shown that visual function is impaired at isoluminance for many different tasks. A significant exception is Sachtler and Zaidi's[1] result that visual memory is superior for chromatic qualities than for gray levels: for short time intervals, memory thresholds for hue and saturation are almost as fine as discrimination thresholds, whereas memory for gray levels is considerably worse than discrimination.[1] This raises the possibility that in the functionally important task of identifying similar objects dispersed across space and/or time, the color attributed to the objects may be vitally useful. Because similar objects may appear against quite dissimilar backgrounds, it is important to note that the memory results in Sachtler and Zaidi[1] concern absolute hue, saturation, and brightness, and not relative qualities that could change depending on the surround. It is also fortuitous that, in variegated scenes, the colors of patches are not influenced by color induction when the surround includes high spatial-frequency chromatic variations.[2]

The paragraph above has glossed over an important problem in the identification task. Because the spectrum of light reflected from a material depends on the spectrum of the illuminant, if the color of an object is solely a function of the spectrum of light reflected from it, the same object should appear of different colors under different illuminants. This could possibly negate the usefulness of color as an identification aid. If, however, the visual system contains a mechanism to "discount the illuminant," identical materials could appear identical across illuminants. This, of course, is the thinking behind the concept called "color constancy."

Most models of color constancy invoke early adaptation mechanisms to equate neural signals from similar materials across different illuminants.[3-8] However, experimental results show that, in variegated scenes, whereas adaptation mechanisms do attenuate the differences between neural signals across illuminants, in general the residual differences are greater than the limen of chromatic discrimination.[9] In addition, a large number of experimental studies have all concluded that object colors as measured by asymmetric matching are not perfectly constant across illuminants.[10-14]

I have previously[15] proposed that it is better to ask new types of questions: Do materials appear to be of "system-

FIG. 1. Sundance.[16] Photograph scanned with an HP Scanjet 4P and printed on a Tektronix Phaser II SD.

atically" different colors under different illuminants? Instead of viewing a failure of constancy as a limitation of the visual system, should it be regarded as a design feature that allows the observer to extract information about illuminants as well as objects? These questions lead to a performance-based concept of color constancy, in which it is important to measure whether observers can recognize that objects are being seen under different illuminants, whether they can identify similar objects across illuminants despite changes in appearance, and whether they can infer the relative colors of the illuminants.

Measurements of this type can be illustrated in the photograph of the hills in Fig, 1.[16] The first question is whether an observer attributes the differences between the colors of the trees in the yellower wedge in the foreground relative to the trees in the rest of the foreground to differences in illumination. The second question is whether an observer is able to identify trees with similar foliage across the two illuminants despite the yellower appearances in the triangular patch. The third question is whether an observer can infer from the relative appearance of the groups of trees that sunlight is falling on the wedge, whereas the rest of the foreground is in shade.

Measurements related to object identification can be operationalized in the psychophysical paradigm presented in Fig. 2. In this paradigm, observers are first shown Fig. 1, made acquainted with the concept of matching foliages across illuminants, and then shown a few examples of Fig. 2. In Fig. 2, the chromaticities of the background ellipses and the four circular test disks were calculated from material reflectance spectra for a sample of 170 everyday objects[17] under two different phases of natural light.[18] Three of the disks represent matching reflectance spectra, whereas the fourth disk is the target. The color of the target disk is set equal to the color of the matching disk under the illuminant on the same side, plus a delta. The delta can be varied in either direction along any color vector, e.g., the difference vector between the chromaticities of the matching objects under the two lights, or the chromatic vector orthogonal to the difference vector. Observers are given the following instructions.

"The situations you will be tested on will have a number of colored elliptical materials present under two different lights. Notice the vertical divide in the middle of the screen between the two lighting conditions, and the difference in colors of ellipses on the two sides. The materials you will be asked to match will be circular disks. Two each will be present under each light. In every presentation three of the disks will be of the same material, and one will be of a different material. You will be asked to indicate which material is different by use of the switch box. In every trial, the same materials under the same light should look roughly the same as each other, but may look quite different under different lights. Different materials should look different even under the same light. In doing this task, you should first judge on which side the two disks look more different, to identify the target side. Then compare the two horizontal across-illuminant pairs to decide which of the two disks on the target side is not the same material as on the other side."

For each test material, the percentage of times the correct side is chosen as a function of length along a delta vector, measures the discrimination ability of the observer. The percentage of time the correct object is chosen, given that the correct side has been chosen, is a measure of the ability of the observer to identify similar materials across illuminants. In this paradigm, if an observer gets the target correct every time the two disks on either side are discriminably different, then identification performance is limited only by discrimination.

There are a number of reasons why this procedure is superior to the conventional method of measuring color constancy by asymmetric matching. First, this method does not make the assumption that similar materials should appear identical across illuminants. Figures 1 and 2 show that this assumption is invalid for simultaneously present illuminants. Informal observations with the display in Fig. 2 showed that the assumption is still invalid when observers view the two halves haploscopically and simultaneously, each eye maintaining separate adaptation. Second, this method puts an observer in the mental set of identifying similar materials, whereas asymmetric color matching would entirely miss the possible ability of an observer to

FIG. 2. Ellipses representing material reflectances[18] under different daylights.[19] Three of the disks represent the same material. Observer's task is to pick the disk that represents a different material. The 36-bit experimental display has been quantized to 24 bits, JPEG compressed, and printed on a Teletronix Phaser IISD.

identify objects despite changes in appearance. Third, on the other hand, if an observer is terrible at identifying similar objects across illuminants, but can perform appearance matching, asymmetric color matches would seriously overestimate color constancy. In other words, just because two patches look identical across illuminants to an observer does not mean that they appear to belong to the same material to that observer, as can also be gleaned from the two studies that have required observers to match stimuli on the basis of inferred object reflectance.[19,20]

The new procedure can be applied to many different situations. In my laboratory, besides the simultaneous illuminants condition (Fig. 2), we are applying it to a haploscopic[21] version of Fig. 2 to simulate successive illuminants, to lightness constancy for real crumpled objects,[22] and to test color scission[23] under transparent layers.[24] My aim in this article is to show the physical and neural reasons why an observer should be able to perform well on the task in Fig. 2 in certain situations ranging from experimental to natural, but not in others. The data from the experiments will appear in future publications.

CORRELATED SHIFTS IN CONE SIGNALS ACROSS ILLUMINANTS

To test whether materials appear to be of "systematically" different colors under different illuminants, Zaidi, Spehar, and DeBonet[9] plotted absorptions for each cone type, L, M, and S from the 170 Vrhel[17] objects under two different daylights.[18] The most noticeable aspect of all these plots was that the points representing individual objects lay close to straight lines, i.e., there was a strong correlation between the quanta absorbed by each cone type from different objects across illumination changes. Comparable correlations also exist for cone absorptions from other samples of objects and illuminants.[9,25,26] These systematic changes in cone absorptions and subsequent neural signals make it possible to devise simple schemes for object and illuminant color identification.[15]

From a different direction, the results above had been presaged by work in computer vision examining the sufficiency of diagonal transforms for color constancy.[27] This work had provided formal proofs that diagonal transforms are sufficient, if surface reflectances can be described by two basis functions and illuminants by three, or reflectances by three and illuminants by two basis functions. Because these are not proofs of necessary conditions, they do not address the sufficiency of other possibilities. In fact, as shown below, a basis function or spectral frequency approach to reflectances[28] may not even be a suitable analysis for the generality of correlated cone absorptions.

In analyzing this problem, I want to exploit the fact that in each of the *L, M, S* plots in Zaidi *et al* [9], the points representing individual objects all lie close to the line joining (0, 0) and the point representing the two illuminants' absorptions. In other words, if for a particular cone absorption spectrum $P(\lambda)$, and two illuminant spectra $I_a(\lambda)$ and $I_b(\lambda)$, the ratio of cone absorptions is a/b, i.e.,

$$\frac{\int P(\lambda)I_a(\lambda)d\lambda}{\int P(\lambda)I_b(\lambda)d\lambda} = \frac{a}{b}. \qquad (1)$$

Then all those objects j, with spectra $\theta_j(\lambda)$, fall on the correlation line whose absorptions are also in the ratio a/b, i.e.,

$$\frac{\int \theta_j(\lambda)\,P(\lambda)I_a(\lambda)d\lambda}{\int \theta_j(\lambda)\,P(\lambda)I_b(\lambda)d\lambda} = \frac{a}{b}. \qquad (2)$$

The requirement in Eq. (2) can be written as the following scalar product:

$$\int \theta_j(\lambda)[P(\lambda)I_a(\lambda)/a - P(\lambda)I_b(\lambda)/b]d\lambda = 0. \qquad (3)$$

Hence, object j falls on the correlation line, if the object spectral reflectance, considered as a vector, is orthogonal to the difference vector in the square-brackets, which is a linear combination of the vectors found by wavelength-by-wavelength multiplication of cone and illuminant spectra. The sum of all components of the difference vector is zero, but its length is positive. The set of $\theta_j(\lambda)$ that satisfy Eq. (3), span a hyperplane passing through the (1,1,1,. . .,1) vector, in the all-positive portion of a space of dimensionality one less than dim(λ).

Figure 3 examines cone absorptions[29] from the 170 objects[17] under Direct Sunlight and Zenith Skylight.[18] The spectra of the two illuminants are shown in Fig. 3(a). Figure 3(b) shows the results of wavelength-by-wavelength multiplication of each of the illuminant spectra with each of the cone spectral sensitivity curves, divided by a or b as is appropriate from Eq. (3). This panel reveals that the major differences between the illuminant spectra are attenuated by multiplication with the cone absorption curves. For each cone type, the curves in Fig. 3(c) show the difference between the two corresponding curves in Fig. 3(b), and represent the difference vectors in Eq. (3). When the illuminant spectra do not contain significant spikes, the wavelength-by-wavelength product curves, normalized to unit area by the division in Eq. (3), are approximately shifted versions of each other, and the difference curves have roughly symmetric shapes. The difference curves are close to zero for a larger number of wavelengths than the corresponding cone-absorption spectra. Consequently, for each difference vector, many different sorts of object spectra yield a sum of wavelength-by-wavelength products with the positive lobe that is roughly equal to the sum with the negative lobe, and, hence, the scalar product is close to zero. In particular, band limiting the frequency of the object spectrum or limiting the number of basis functions would be irrelevant, because a spectrum consisting of any high fre-
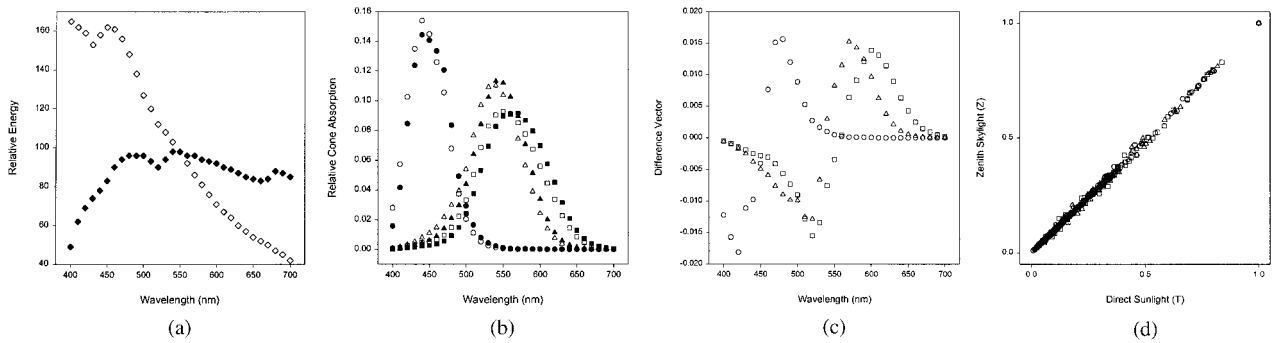
(a)　　　　　(b)　　　　　(c)　　　　　(d)

FIG. 3. (a) Energy spectra of illuminants: (closed symbols) T = Direct Sunlight and (open symbols) Z = Zenith Skylight.[18] (b) Wavelength-by-wavelength multiplication of cone absorption spectra.[29] (L = squares, M = triangles, S = circles) with the spectra of (closed symbols) illuminant T and (open symbols) illuminant Z. (c) Differences between the pairs of curves for each cone type in Fig. 3(b). These difference spectra (L = squares, M = triangles, S = circles) correspond to the difference vectors in Eq. (3). (d) Excitation of L, M, S cones (L = squares, M = triangles, S = circles) from each of 170 objects[17] under illuminants T and Z. The points at (1.0, 1.0) represent cone absorptions from the two illuminants.

quency sinusoid gives a scalar product of zero. In Fig. 3(d), the same cone class symbols are used to plot all the cone absorptions from the 170 objects under Direct Sunlight vs. Zenith Skylight. The absorptions from the illuminants are used to normalize each set to a maximum of 1.0, so that the overlapped points on the top-right corner represent the illuminants' cone absorptions. Notice that almost all object absorptions fall along or close to a straight line between (0,0) and the illuminants' absorptions. The slope of each point gives the ratio corresponding to the LHS of Eq. (2) (a/b is normalized to 1.0). Significant departures of ratios from 1.0 were generally limited to objects with very low cone absorptions. This conclusion is expectedly different from that reached by examining departures from zero of projections of $\theta_j(\lambda)$ on the difference vectors,[6] i.e., of the Fourier coefficients calculated by dividing the LHS of Eq. (3) by the squared norm of the difference vector. As shown in the next section, ratios are more germane to algorithms that exploit across-illuminant correlations as physical invariants.

Correlations similar to Fig. 3(d) are found for almost all illuminant pairs and cone absorptions tested, but, because of space constraints, just two more examples are shown. Figure 4 shows what was expected to be a pathological case. Cone absorptions are compared for Skylight[18] vs. a Flourescent lamp, which has spikes in its energy spectrum.[30] How-

ever, again the scalar products of object reflectances with the difference vectors were close to zero and cone absorptions were highly correlated across the illuminants. This is despite the fact that the spectrum of the Flourescent light contains high-frequency components. The large positive spikes in Fig 4(c) are balanced by the larger number of moderate negative values, and the curves are close to zero for many wavelengths. Consequently, almost all the scalar products are close to zero, despite significant differences in cone absorptions from different objects across illuminants.

Figure 5 compares cone absorptions under Skylight[18] and a Tungsten Lamp,[30] and illustrates possibly the lowest correlated changes found, as shown by the scatter in the correlation graphs [Fig. 5(d)]. The form of the correlation is similar to the other graphs, and the correlation is still extremely high, but objects that are distinct under one illuminant become metamers under the other and vice versa.[30] It is worth noting that, on the energy vs. wavelength plot, the spectrum of Tungsten light is almost orthogonal to the spectrum of Skylight [Fig. 5(a)].

AFFINE TRANSFORMS ALONG CARDINAL CHROMATIC DIRECTIONS

Cone signals are recoded into two chromatically opponent signals in the eye, and these signals are transmitted to the
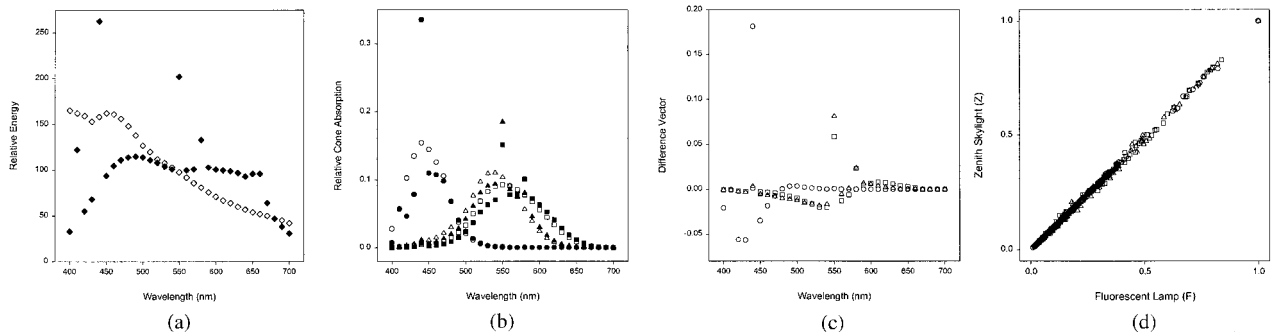

(a)　　　　　(b)　　　　　(c)　　　　　(d)

FIG. 4. Similar to Fig. 3 for cone absorptions under (open symbols) illuminant Z and (closed symbols) Flourescent Lamp F.[27]
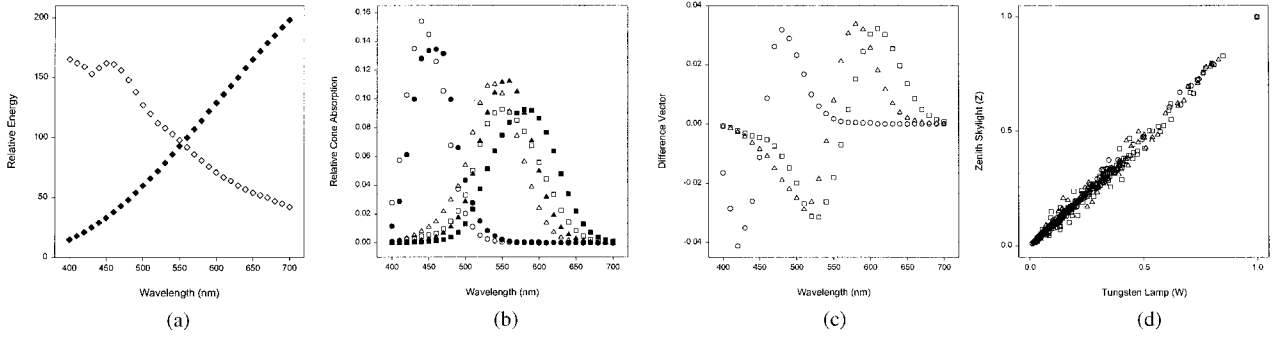
FIG. 5.   Similar to Fig. 3 for cone absorptions under (open symbols) illuminant Z and (closed symbols) Tungsten Lamp W.[27]

cortex.[31] These signals are represented on the cardinal $rg = L/(L + M)$ and $yv = S/(L + M)$ axes of the MacLeod–Boynton equiluminant color space.[32,33] Zaidi *et al.*[9] found that, to a good approximation for all pairs of changes between phases of natural daylight, object chromaticities were shifted additively along the *rg* axis and multiplicatively along *yv*. To exploit the mathematical invariants of affine transforms, these changes can be represented in the form:

$$\begin{bmatrix} rg_{ja} \\ yv_{ja} \end{bmatrix} = \begin{bmatrix} 1 & 0 \\ 0 & \sigma_{ab} \end{bmatrix} \begin{bmatrix} rg_{jb} \\ yv_{jb} \end{bmatrix} + \begin{bmatrix} \tau_{ab} \\ 0 \end{bmatrix} \qquad (4)$$

where *j* is the index for objects in the sample; (rg_{ja}, yv_{ja}) and (rg_{jb}, yv_{jb}) are the $L/(L + M)$ and $S/(L + M)$ chromaticities of the object under illuminants I_a and I_b, respectively; and (τ_{ab}, σ_{ab}) describe the shift in the chromaticities (rg_a, yv_a) of I_a relative to the chromaticities (rg_b, yv_b) of I_b, i.e.,

$$\begin{bmatrix} rg_a \\ yv_a \end{bmatrix} = \begin{bmatrix} 1 & 0 \\ 0 & \sigma_{ab} \end{bmatrix} \begin{bmatrix} rg_b \\ yv_b \end{bmatrix} + \begin{bmatrix} \tau_{ab} \\ 0 \end{bmatrix}. \qquad (5)$$

Equation (4) follows from two empirically established generalizations. First, given the high correlations between cone absorptions from objects across illuminants, as a good approximation, we can write for all *j*:

$$\mathbf{L_{ja}} = \alpha \mathbf{L_{jb}}; \; \mathbf{M_{ja}} = \beta \mathbf{M_{jb}}; \; \mathbf{S_{ja}} = \gamma \mathbf{S_{jb}}. \qquad (6)$$

Second, Zaidi[34] showed that for Vrhel objects under the same illuminant, the correlation between L cone absorption and M cone absorption is around 0.99, but the correlations between L and S and M and S are low. Therefore, as a good approximation, we can also write:

$$\mathbf{L_{ja}} = \nu \mathbf{M_{ja}}; \; \mathbf{L_{jb}} = \omega \mathbf{M_{jb}}. \qquad (7)$$

Given these conditions,

$$\tau_{ab} = \frac{L_{ja}}{L_{ja} + M_{ja}} - \frac{L_{jb}}{L_{jb} + M_{jb}} = \frac{\omega(\alpha - \beta)}{(\alpha\omega + \beta)(\omega + 1)}. \qquad (8)$$

The difference ($yv_{ja} - yv_{jb}$) does not reduce to a constant from Eqs. (6) and (7), but

$$\sigma_{ab} = \frac{S_{ja}}{L_{ja} + M_{ja}} \bigg/ \frac{S_{jb}}{L_{jb} + M_{jb}} = \frac{\gamma(\omega + 1)}{(\alpha\omega + \beta)}. \qquad (9)$$

The chromaticities for any object *j* follow the affine trans-

form in Eq. (4) to the extent that Eqs. (6) and (7) hold for that particular object.

The affine transform in Eq. (4) was used to devise heuristic-based algorithms that solve the correspondence problem for materials across illuminants and simultaneously infer the relative chromaticities of the illuminants.[15] An example of one class of situations in which the algorithm was successful, is depicted in Fig, 6. The central panel shows the chromaticities of 17 randomly chosen surfaces under Equal Energy light. Chromaticities of a random subset of 6 of these under Zenith Skylight are shown in the left panel as crosses. The scenario is that the algorithm has access only to the two sets of chromaticities, as if a subset of the objects were present under a different light and in possibly a different spatial arrangement. The affine transformation assumption implies that the shape formed by the crosses should be similar to the shape formed by the circles belonging to the same materials, subject to a translation along the horizontal axis, and an expansion or compression along the vertical axis. The algorithm tries to find the best template match between discrete points for these transformations. The panel on the right shows the transformed crosses along with the correct target circles, demonstrating that the correspondence problem is solved correctly. The small mismatches do not matter, because the algorithm identifies discrete pairs of corresponding objects. In addition, the transformation automatically provides the illuminant chromaticity shift. The success of the algorithm validates the affine transformation assumption.

AFFINE TRANSFORMS FOR ROUGH SURFACES

The situation above assumes that each object is well represented by a single pair of *(rg,yv)* chromaticities. This assumption is valid for Lambertian surfaces of unvarying spectral reflectance lit by a uniform illuminant. However, most objects in the world have more complex surfaces. Observations of real-world textured objects reveal that there are point-by-point changes in appearance, the same surface appears of a different color where it is smooth than where it is rough, and the variations of roughness give a clue as to the specularity of the substance and its metallic/nonmetallic nature. In fact, source-object-sensor geometry at each point
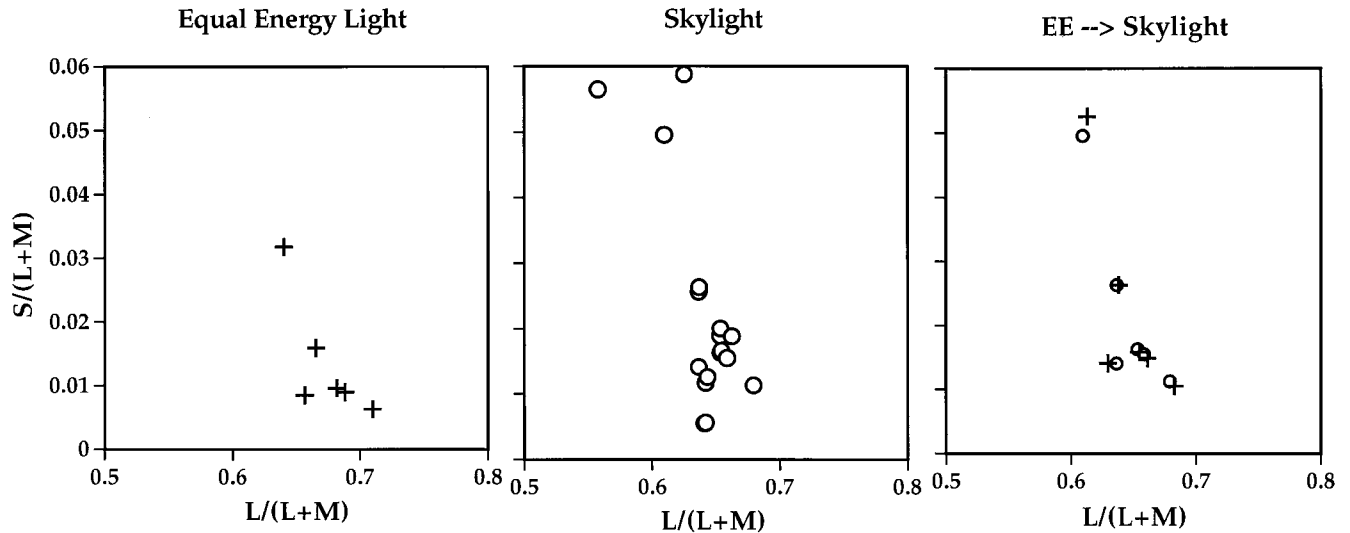
Recovery of Lambertian Objects

FIG. 6. Matching of materials by the affine-heuristic algorithm despite illuminant-caused chromaticity shifts. Left: Chromaticities of 6 Lambertian objects[17] under equal-energy light. Center: Chromaticities of 17 Lambertian objects[17] under skylight. The 6 objects in the left panel are included in the 17. Right: Crosses represent results of applying to the crosses in the left panel the best affine transformation calculated by the algorithm. To show the accuracy of the matching procedure, circles for the same objects are replotted from the center panel.

of the surface determines the absolute and relative magnitudes of the interface reflection (which has the same spectrum as the illuminant), and the body reflection (which is a wavelength-by-wavelength multiplication of the object and illuminant spectra). When surfaces have a rough microstructure, both interface and body reflections are diffuse. The intensity of interface reflection has a peak at an angle forward of the specular.[35] The intensity of body reflection has a peak in the direction of the source and is more diffuse for rougher surfaces.[36] For plastics, and other inhomogeneous dielectric materials, even smooth surfaces are non-Lambertian for oblique illumination.[37] The colors and shapes of highlights also depend on the surface roughness.[36]

To test the algorithm's performance for more realistic rough surfaces, the first case tackled is where the source-object-sensor geometry is constant across two illuminants, but where rough surfaces are present in different parts of the scene in arbitrary facets. In that case, for both illuminants, the total reflection from each surface facet can be expressed as an invariant weighted sum of the body and the interface
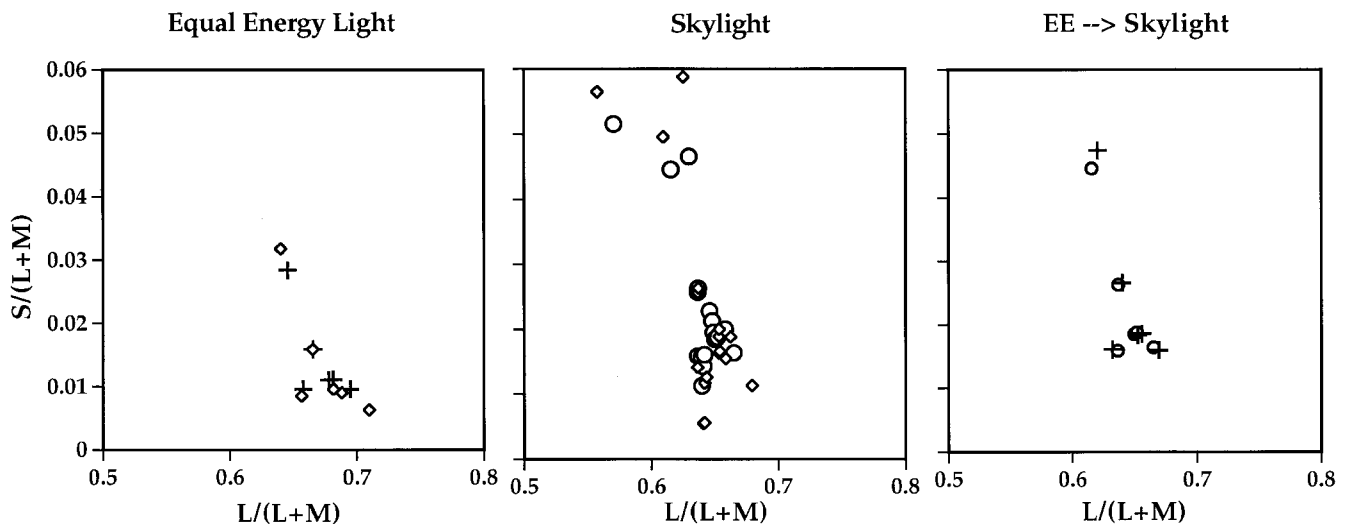
Recovery of Rough Objects in Random Facets

FIG. 7. Same as for Fig. 6, but for rough surfaces. Diamonds in the left and center panels represent body reflections chromaticites, "+" and "o" in these panels are chromaticity shifts caused by mixture with the interface reflection.
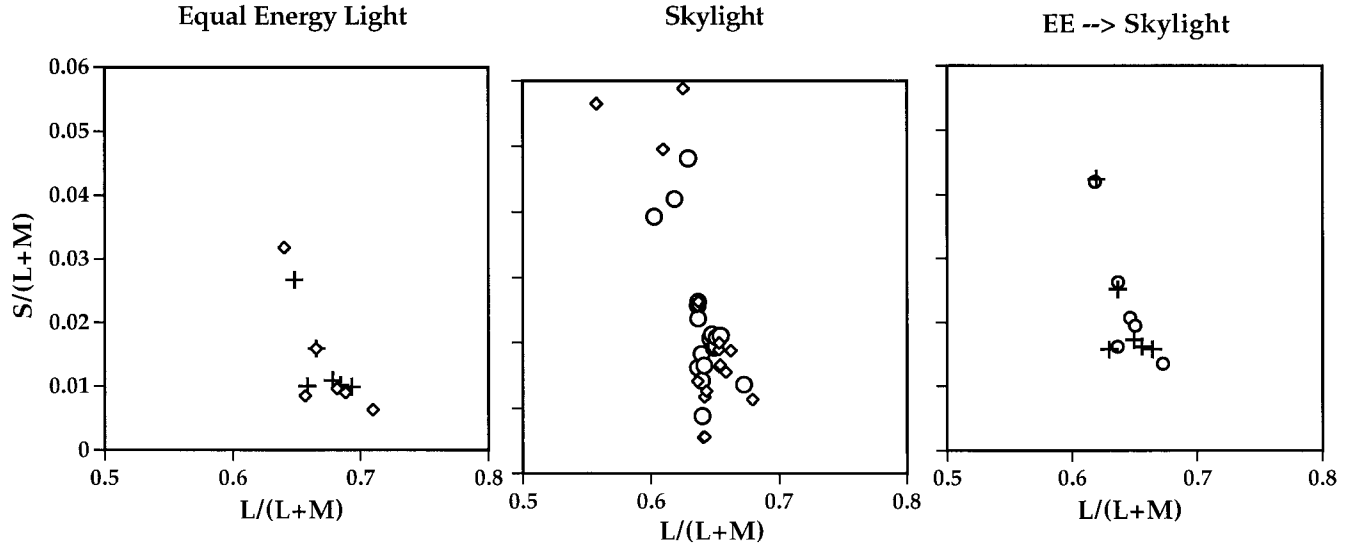
FIG. 8. Same as Fig. 7, except that each of the objects is present under the first light in a different facet than under the second.

reflection, i.e., for each illuminant I_i, the chromaticity (RG_{ji}, YV_{ji}) of the total reflection is an invariant weighted sum of the chromaticity of the body reflection (rg_{ji}, yv_{ji}) and the illuminant chromaticity (rg_i, yv_i). In that case, the chromaticities of the total reflections obey the same affine transformation as the illuminant and body reflection chromaticities. It is reasonable to make the assumption[36] for each facet of a rough object that:

Total Reflection $= k$ (Body Reflection)

$$+ (1 - k) \text{ (Interface Reflection),} \quad (10)$$

i.e., for each illuminant I_i:

$$\begin{bmatrix} RG_{ji} \\ YV_{ji} \end{bmatrix} = k \begin{bmatrix} rg_{ji} \\ yv_{ji} \end{bmatrix} + (1 - k) \begin{bmatrix} rg_i \\ yv_i \end{bmatrix}. \quad (11)$$

Then, substituting Eqs. (4) and (5) into Eq. (11) and gathering terms:

$$\begin{bmatrix} RG_{ja} \\ YV_{ja} \end{bmatrix} = \begin{bmatrix} 1 & 0 \\ 0 & \sigma_{ab} \end{bmatrix} \begin{bmatrix} RG_{jb} \\ YV_{jb} \end{bmatrix} + \begin{bmatrix} \tau_{ab} \\ 0 \end{bmatrix}. \quad (12)$$

Figure 7 shows a simulation of the algorithm for the same objects as in Fig. 6. In this simulation, each of these objects is assumed to consist of a homogeneously rough material, and the objects are present in random facets, but in the same facets under the two illuminants. This would be the case, if the spectrum of the illuminant changed over a fixed scene. Hence, the value of k in Eq. (11) is less than 1.0 for all objects, and is chosen at random for each object but identical under both illuminants. The small diamonds in the left and center panels represent the body chromaticities under Skylight and Equal-Energy lights, and are identical to the circles and pluses in Fig. 6. The pluses and circles represent the total reflection chromaticities and are shifted towards the

illuminant chromaticities. The right panel shows that, in this case, the algorithm solves the correspondence problem as successfully as in Fig. 6.

A more difficult case is depicted in Fig. 8, where objects are present in different spatial arrangements under the two illuminants, i.e., the source-object-sensor geometry represented by the value of k for each object is randomized across the illuminants. In this case, Eq. (12) is not valid; therefore, the algorithm should not be expected to solve the correspondence problem. The right panel shows mismatches between the transformed pluses and the target circles.

There is an important difference between Figs. 7 and 8. In Fig. 7, mixtures of the interface reflection with the body reflection lead to distortions in the shapes formed by the chromaticities in the left and center panels, but the distortions are similar, so the algorithm is successful. In Fig. 8, the distortion in the left panel can be very dissimilar from the distortion in the center panel, and the algorithm is not designed to correct for this change. The results of a large

FIG. 9. Center panel: A cylindrical surface made out of a rug.[38,39] Left and right panels: Strips isolated from the cylinder.
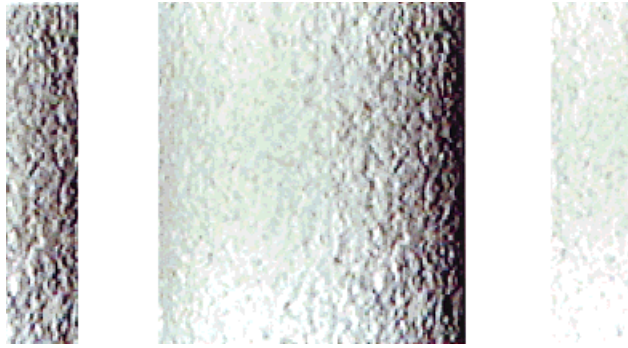
FIG. 10. Similar to Fig. 9 for a plaster cylinder.

number of simulations for the three different situations represented by Figs. 6, 7, and 8 have shown that the algorithm is very robust in the first two situations: the initial object chosen by the algorithm to be matched does not influence the final solution appreciably. On the other hand, the algorithm is very susceptible to the starting point for the situation in Fig. 8.

The task in Fig. 8, however, is one that the human visual system also does not seem to be able to perform. In the center of Fig. 9 is a cylinder from the Columbia–Utrecht database,[38,39] constructed from photographs of a rug taken in different facets. On the two sides are narrow strips extracted from this cylinder. Even though the two strips are actually the same material as seen in two different facets under the same illuminant, they do not appear to be the same color or even the same material. Figure 10 demonstrates that this judgment is also difficult for achromatic objects. This cylinder from the Columbia–Utrecht database was constructed from facets of a piece of plaster. In the absence of stereo information, the two extracted narrow strips on the sides do not seem to have the same roughness or albedo.

SUMMARY

In this article, I have espoused a performance-based view of color constancy, in which the task for the observer is to identify similar materials across illuminants despite possible appearance changes, and to simultaneously extract the relative colors of the illuminants. I have shown the physical and neural constraints on chromatic signals that make it possible to use simple heuristic-based algorithms to accomplish these tasks in certain situations.

An affine-heuristic algorithm can solve the correspondence problem for most Lambertian surfaces in random spatial arrangements under different illuminants. For rough surfaces, where the relative amounts of interface and body reflections vary with source-object-sensor geometry, the algorithms solve the correspondence problem across illuminants for a constant source-object-sensor geometry. The algorithms are not successful for rough surfaces in random spatial arrangements under different illuminants. However, in real-world situations, three-dimensional objects sometimes share enough visible facets across scenes and illuminants, so that color identification algorithms could be useful when combined with recognition of other object properties.[40]

1. Sachtler W, Zaidi Q. Chromatic and luminance signals in visual memory. J Opt Soc Am A 1992;9:877–894.
2. Zaidi Q, Yoshimi B, Flanigan N, Canova A. Lateral interactions within color mechanisms in simultaneous induced contrast. Vision Res 1992; 32:1695–1707.
3. Ives HE. The relation between the color of the illuminant and the color of the illuminated object. Trans Illum Eng Soc 1912;7:62–72. Reprinted in: Color Res Appl 1995;20:70–75.
4. Land E, McCann JJ. Lightness and retinex theory. J Opt Soc Am 1971;61:1–11.
5. Land E. Recent advances in retinex theory and some implications for cortical computations: color vision and the natural image. Proc Natl Acad Sci (USA) 1983;80:5163–5169.
6. West G, Brill MH. Necessary and sufficient conditions for Von Kries chromatic adaptation to give color constancy. J Math Biol 1982;15: 249–258.
7. Dannemiller JL. Computational approaches to color constancy: adaptive and ontogenetic considerations. Psych Rev 1989;96:255–266.
8. Brill MH. Image segmentation by object color: a unifying framework and connection to color constancy. J Opt Soc Am A 1990;7:2041–2049.
9. Zaidi Q, Spehar B, DeBonet JS. Color constancy in variegated scenes: the role of low-level mechanisms in discounting illumination changes. J Opt Soc Am A 1997;14:2608–2621.
10. Valberg A, Lange–Malecki B. 'Colour constancy' in Mondrian patterns: a partial cancellation of physical chromaticity shifts by simultaneous contrast. Vision Res 1990;30:371–380.
11. Walraven J, Benzshawel TL, Rogowitz BE, Lucassen MP. Testing the contrast explanation of color constancy. In: Valberg A, Lee B, editors, From pigments to perception. New York: Plenum; 1991. p 369–378.
12. Helson H, Judd D, Warren M. Object-color changes from daylight to incandescent filament illumination. Illum Eng 1952;47:221–233.
13. McCann J, McKee S, Taylor T. Quantitative studies in retinex theory. Vision Res 1976;16:445–458.
14. Brainard DH. Color constancy in the nearly natural image. 2. Achromatic loci. J Opt Soc Am A 1998;15:307–325.
15. Zaidi Q. Identification of illuminant and object colors: heuristic-based algorithms. J Opt Soc Am A 1998;15:1767–1776.
16. Ketchum RG. The legacy of wilderness: The photographs of Robert Glenn Ketchum. New York: Aperture Foundation; 1993.
17. Vrhel M, Gershon R, Iwan LS. Measurement and analysis of object reflectance spectra. Color Res Appl 1994;19:4–9.
18. Taylor AH, Kerr GP. The distribution of energy in the visible spectrum of daylight. J Opt Soc Am 1941;31:3.
19. Marzynski G. Z Ps 1921;87:45–72. (Described in: Woodworth RS. Experimental Psychology. Henry Holt; 1939).
20. Arend LE, Reeves R. Simultaneous color constancy. J Opt Soc Am A 1986;3:1743–1751.
21. Bramwell DI, Hurlbert AC. Measurements of colour constancy by using a forced-choice matching technique. Perception 1996;25:229–241.
22. Robilotto R, Zaidi Q. Performance based lightness constancy: crumpled 3D objects. Investig Ophthal Vis Sci 2000;41:S227.
23. D'Zmura M, Colantoni P, Knoblauch K, Laget B. Color transparency. Perception 1997;26:471–492.

24. Khang B, Zaidi Q. Tests of color scission by identification of transparent overlays. Investig Ophthal Vis Sci 2000;41:S239.
25. Dannemiller JL. Rank ordering of photoreceptor catches from objects are nearly illumination invariant. Vision Res 1993;33:131–137.
26. Foster DH, Nascimento SMC. Relational colour constancy from in variant cone-excitation ratios. Proc R Soc London Ser B 1994;250:116–121.
27. Finlayson GD, Drew MS, Funt BV. Color constancy: generalized diagonal transforms suffice. J Opt Soc Am A 1994;11:3011–3019.
28. Maloney L. Evaluation of linear models of surface spectral reflectance with small numbers of parameters. J Opt Soc Am A 1986;3:1673–1683.
29. Smith VC, Pokorny J. Spectral sensitivity of the foveal cone photopigments between 400 and 700 nm. Vision Res 1975;15:161–171.
30. Wyszecki G, Stiles WS. Color science. New York: Wiley; 1982.
31. Derrington AM, Krauskopf J, Lennie P. Chromatic mechanisms in lateral geniculate nucleus of macaque. J Phys 1984;357:241–265.
32. MacLeod DIA, Boynton RM. Chromaticity diagram showing cone excitation by stimuli of equal luminance. J Opt Soc Am 1979;69:1183–1186.
33. Krauskopf J, Williams DR, Heeley D. Cardinal directions of color space. Vision Res 1982;22:1123–1131.
34. Zaidi Q. Decorrelation of L and M cone signals. J Opt Soc Am A 1997;14:3430–3431.
35. Torrance KE, Sparrow EM. Theory for off-specular reflection from roughened surfaces. J Opt Soc Am 1967;57:1105–1114.
36. Oren M, Nayar SK. Generalizations of the Lambertian model and implications for machine vision. Int J Comp Vis 1995;14:227–251.
37. Wolff LB. A diffuse reflectance model for smooth dielectrics. J Opt Soc Am A 1994;11:2956–2968.
38. Dana KJ, Ginneken B, Nayar SK, Koenderink JJ. Reflectance and texture of real-world surfaces. Columbia University Technical Report CUCS-046-96.
39. Dana KJ, Ginneken B, Nayar SK, Koenderink JJ. Reflectance and texture of real-world surfaces. Columbia University Technical Report CUCS-048-96.
40. Gegenfurtner KR. Sensory and cognitive contributions of color to the recognition of natural scenes. Investig Ophthal Vis Sci 1998;39:S156.